Available online at www.sciencedirect.com

Catalysis Today 87 (2003) 11–17

CATALYSIS TODAY

www.elsevier.com/locate/cattod

Selective oxidation of hydrogen sulfide over mixture catalysts of V–Sb–O and Bi_2O_3

Bong-Guk Kim [a], Dae-Won Park [a,*], Il Kim [a], Hee-Chul Woo [b]

[a] *Division of Chemical Engineering, Pusan National University, Kumjeong-ku, Busan 609-735, South Korea*
[b] *Department of Chemical Engineering, Pukyung National University, Busan 608-739, South Korea*

Abstract

The selective oxidation of hydrogen sulfide containing excess water and ammonia was studied over vanadium–antimony mixed oxide catalysts. The investigation was focused on the phase cooperation between V–Sb–O and Bi_2O_3 in this reaction. Strong synergistic phenomenon in catalytic activity was observed for the mechanically mixed catalysts of V–Sb–O and Bi_2O_3. Temperature-programmed reduction (TPR) and oxidation (TPO), two separated bed reaction tests, and XPS analyses were carried out to explain this synergistic effect by the reoxidation ability of Bi_2O_3.

Keywords: Hydrogen sulfide; Selective oxidation; Phase cooperation; Vanadium–antimony mixed oxide

---

1. Introduction

Since the international environmental regulations concerning the release of sulfur containing gas become more stringent, hydrogen sulfide contained in the acid gases should be effectively recovered before emission to atmosphere. For many years, most of hydrogen sulfide in petroleum refineries and natural gas plants has been removed by the well-known Claus process [1,2]. The Claus process consists of two steps: thermal oxidation and catalytic reaction. In the thermal oxidation, one-third of H_2S is first burned with air to produce sulfur dioxide in a waste heat furnace, while unconverted H_2S reacts with SO_2 to elemental sulfur through the subsequent catalytic reaction over Al_2O_3 catalysts. However, due to thermodynamic limitations, 3–5% of H_2S is typically not converted to sulfur. More than 25 tail gas clean-up processes have been developed using dry solids or wet absorption methods to improve the overall sulfur recovery efficiency from Claus plants. Most of the technology options have been reviewed [3]. Among the various processes, Sulfreen [4], Clauspol [5] and SCOT [6] are widely used ones. Recently, a dry catalytic process has been developed for the selective catalytic oxidation of H_2S to elemental sulfur. Examples of commercially developed catalysts for this purpose are the titanium-based catalysts in the MODOP process [7,8] and the iron-based catalysts in the Super Claus process [9–11]. In the MODOP process, H_2S is oxidized into elemental sulfur with a stoichiometric amount of oxygen over TiO_2 catalysts. One drawback of the MODOP process is that water should be removed from the tail gas before the reaction, due to the deactivation of catalysts in the presence of water. In the Super Claus process, tail gas can be treated without a dehydration step, since the Fe_2O_3/SiO_2 catalyst is not deactivated even in the presence of 30 vol.% of water vapor. However, the Super Claus process cannot

---

[*] Corresponding author. Tel.: +82-51-510-2399;
fax: +82-51-512-8563.
E-mail address: dwpark@pusan.ac.kr (D.-W. Park).

0920-5861/$ – see front matter © 2003 Elsevier B.V. All rights reserved.
doi:10.1016/j.cattod.2003.10.007

treat high concentrations of H_2S above 2 vol.% because it is necessary to supply excess oxygen (usually 10 times the stoichiometric amount) to overcome the catalytic deactivation caused by water.

Hydrogen sulfide in the coke oven gas released from the steel smelting process is scrubbed and concentrated using aqueous ammonia solution. Concentrated H_2S that is separated from aqueous ammonia is transferred to the Claus plant to convert it into elemental sulfur, and remaining aqueous ammonia is usually incinerated. However, the separation of H_2S from the aqueous ammonia is not perfect. Remaining aqueous ammonia stream contains about 2% H_2S which in turn causes the SO_x emission problem during the incineration. In this case, the control of SO_x emission is difficult because the stream contains not only excess water vapor but also high concentration of ammonia.

One approach to resolve the problem is the selective catalytic oxidation of H_2S to ammonium thiosulfate (ATS) and elemental sulfur as reported in our previous works [12,13]. We reported a new vapor phase catalytic process for the selective conversion of H_2S in a stream containing both ammonia and water. V_2O_5/SiO_2, Fe_2O_3/SiO_2 and Co_3O_4/SiO_2 catalysts showed good catalytic activities in the selective oxidation of H_2S to ATS and sulfur. Vanadium–antimony catalyst has recently been studied for the oxidation of hydrogen sulfide to elemental sulfur in the absence of ammonia [14]. We reported improved performance of V–Sb–O/TiO_2 compared to V_2O_5/TiO_2 in the selective oxidation of H_2S to ATS and sulfur [13]. The role of Bi_2O_3 in the phase cooperation of binary mixed oxide systems have been widely studied and well reviewed by Weng and Delmon [15]. Mechanical mixtures of two metal oxides can offer much information about the phase cooperation. The conventional process for the production of ATS are based on the liquid phase reactions. The ATS Claus tail gas clean-up process [16] is divided into two sections: absorption of SO_2 from incinerator in aqueous ammonia and conversion of the intermediate product to ATS by sparging H_2S into the converter. In another ATS process [17], sulfuric acid is reacted with aqueous ammonia solution below 45 °C, then the mixture is contacted with H_2S to form ATS. Therefore, our process has an advantage of direct vapor phase operation compared to the above two processes.

In this study, we further examined the performance of vanadium–antimony mixed oxide catalysts for the selective oxidation of H_2S in the stream containing both ammonia and water. Mechanical mixtures of V–Sb–O and Bi_2O_3 were prepared and used to understand the phase cooperation of metal oxides in the oxidation of H_2S. Solid-state modifications of the mixtures during the catalytic reaction tests were verified by characterization before and after the test by XRD and XPS. Temperature-programmed techniques (TPR and TPO) and two separated bed operations were used to elucidate the redox properties of this catalyst system.

2. Experimental

2.1. Catalyst preparation

V–Sb–O catalyst was prepared by a coprecipitation method using ammonium metavanadate (NH_4VO_3, Junsei) and antimony oxide (Sb_2O_3, Merck) as precursors. A 5 wt.% oxalic acid was used to dissolve the precursors. After evaporation at 80 °C, samples were dried at 110 °C overnight and calcined at 500 °C for 5 h. The mechanical mixture catalysts were prepared according to the literature [15]. The V–Sb–O and Bi_2O_3 (Junsei, SA $= 0.69\,m^2/g$) were dispersed in *n*-pentane (Merck, analytical purity). The suspension was stirred in an ultrasonic vibrator (Brasonic 32) for 10 min. *n*-Pentane was evaporated with agitation at 25 °C under vacuum. The remaining *n*-pentane was removed by drying in air at 80 °C for 20 h. Then, the sample was dried at 110 °C overnight and calcined at 500 °C for 5 h. The catalyst was designated as V–Sb–O + Bi_2O_3 (x:y), where x and y represent the weight ratio of V–Sb–O and Bi_2O_3, respectively.

2.2. Reaction test

Reaction tests were carried out in a continuous flow fixed-bed reactor. The reactor was made of a Pyrex® tube with an i.d. of 0.0254 m. A condenser was attached at the effluent side of the reactor, and its temperature was held at 110 °C to condense only solid products (sulfur + ammonium thiosulfate). A line filter was installed after the condenser to trap any solid mist which had not been captured by the condenser.

From the condenser up to gas chromatography, all the lines and fittings were heated above 120 °C to prevent condensation of water vapor. The flow rates of gases were controlled by a mass flow controller (Brooks MFC 5850E). Water vapor was introduced to the reactant stream using an evaporator filled with small glass beads, and its amount was controlled by a syringe pump.

The content of the effluent gas (H_2S, SO_2, and NH_3) was analyzed by a gas chromatography (HP 5890) equipped with a thermal conductivity detector and a 1.83 m Porapak T column (80–100 mesh) at 100 °C. The exit gas from the analyzer was passed through a trap containing a concentrated NaOH solution and vented out to a hood. The solid products (ATS and sulfur) were dissolved in distilled water to separate them, and were weighed individually after drying in vacuum oven at 110 °C. The conversion of H_2S (X) and the selectivity to a special product (SO_2, S, ATS) (S) are defined as follows:

$$X\,(\%) = \frac{[H_2S]_{\text{inlet}} - [H_2S]_{\text{outlet}}}{[H_2S]_{\text{inlet}}} \times 100$$

$$S\,(\%) = \frac{[\text{product}]_{\text{outlet}}}{[H_2S]_{\text{inlet}} - [H_2S]_{\text{outlet}}} \times 100$$

For the calculation of ATS selectivity, moles of ATS was multiplied by a factor of 2 because 1 mol of ATS can be obtained from 2 mol of H_2S.

2.3. Characterization of catalysts

The surface areas of the individual oxides and their mechanical mixtures were measured by N_2 adsorption method using the BET technique (Micromeritics ASAP 2000). The phase analysis was performed by X-ray diffraction crystallography with Cu Kα radiation (Rigaku, DMAX 2400). The 2θ range between 5° and 90° was scanned at a rate of 2°/min. Identification of the phases was carried out by using JCPDS database. XPS analyses were performed with a X-ray photoelectron spectrometer (VG, ESCALAB 220) with monochromatic Al Kα radiation. The samples were pressed into self-supporting wafers without any binder followed by a pretreatment at an ultrahigh vacuum. The binding energies were calculated using the C 1s band as reference (284.6 eV). In order to investigate the phase cooperation mechanism, TPR was carried out. Before reduction, samples were pretreated by heating under air flow from 25 to 450 °C at a heating rate of 10 °C/min. Reduction was achieved under a H_2/N_2 gas mixture (10 vol.% H_2). Gas flow was 20 ml/min and temperature program was from 25 to 700 °C at a heating rate of 10 °C/min. The amount of consumed H_2 was detected by mass spectroscopy (VG Quadrupole). After TPR experiment, the same sample was instantly tested in TPO under 2.5 vol.% O_2 with helium gas balance.

3. Results and discussion

3.1. Catalytic activity of mixture catalysts (V–Sb–O and Bi_2O_3)

Mechanical mixture catalysts of V–Sb–O and Bi_2O_3 are used to study the phase cooperation phenomena with a reactant composition of 5 vol.% H_2S, 2.5 vol.% O_2, 5 vol.% NH_3, 60 vol.% H_2O and the balance helium. The weight ratios of V–Sb–O/Bi_2O_3 were 1/0, 3/1, 1/1, 1/3, and 0/1. Table 1 shows the H_2S conversion and SO_2 selectivity for these catalysts at 260 °C with GHSV of 12,000 h^{-1}. The addition of Bi_2O_3 into V–Sb–O increased H_2S conversion. All the mechanical mixture catalysts (V–Sb–O + Bi_2O_3) showed higher H_2S conversion than the arithmetic average conversion (calculated from the weight ratio and H_2S conversion of V–Sb–O and pure Bi_2O_3). A strong synergy existed between V–Sb–O and Bi_2O_3. V–Sb–O + Bi_2O_3 (1:3) showed the highest value of H_2S conversion (89.9%). The increase of Bi_2O_3 in the mixture catalyst increased sulfur selectivity, but decreased ATS selectivity. Sulfur is well known to be produced by the selective oxidation of H_2S by reactions (1) and (4) for the following Claus process

Table 1
Conversion of H_2S and product selectivity at 260 °C after 8 h of reaction

Catalyst	$X(H_2S)$ (%)	$S(SO_2)$ (%)	S(S) (%)	S(ATS) (%)
V–Sb–O	81.0	0.0	57.4	42.6
V–Sb–O + Bi_2O_3 (3:1)	83.3	0.0	67.0	33.0
V–Sb–O + Bi_2O_3 (1:1)	85.5	0.0	74.5	25.5
V–Sb–O + Bi_2O_3 (1:3)	89.9	0.0	75.8	24.2
Bi_2O_3	68.1	0.0	82.4	17.6

reactions:

$$H_2S + \frac{1}{2}O_2 \rightarrow \frac{1}{n}S_n + H_2O \quad (1)$$

$$\frac{1}{n}S_n + O_2 \rightarrow SO_2 \quad (2)$$

$$H_2S + \tfrac{3}{2}O_2 \rightarrow SO_2 + H_2O \quad (3)$$

$$2H_2S + SO_2 \leftrightarrow \frac{3}{n}S_n + 2H_2O \quad (4)$$

Previous works [18,19] reported that the reaction of SO_2 with NH_3 occurred to form ammonium sulfite, and it was accelerated by the presence of water vapor:

$$SO_2 + 2NH_3 + H_2O \rightarrow (NH_4)_2SO_3 \quad (5)$$

Ammonium thiosulfate (ATS) is commercially produced by the reaction of ammonium sulfite with excess sulfur [20]:

$$(NH_4)_2SO_3 + S \rightarrow (NH_4)_2S_2O_3 \quad (6)$$

ATS can also be produced by the reaction of ammonium sulfide [21], ammonium sulfite, and SO_2:

$$H_2S + 2NH_3 \rightarrow (NH_4)_2S \quad (7)$$

$$(NH_4)_2SO_3 + 2(NH_4)_2S + 3SO_2 \rightarrow 3(NH_4)_2S_2O_3 \quad (8)$$

Therefore, one can see that V–Bi–O is more favorable for the reaction (5), (6) or (8) than Bi_2O_3. However, for all the mixture catalysts zero SO_2 selectivity was observed due to the reaction of SO_2 formed by Eqs. (2) and (3) with NH_3.

A typical temperature dependence of the H_2S conversion and SO_2 selectivity for V–Sb–O + Bi_2O_3 (1:3) catalyst and V–Sb–O is shown in Fig. 1. The H_2S conversion for the mixture catalysts showed maximum at 260 °C. Over the whole temperature ranges, 220–320 °C, the mixture catalyst exhibited higher H_2S conversion than V–Sb–O. The SO_2 selectivities for the mixture catalyst were also lower than V–Sb–O. Thus, the synergy for the mixture catalyst was confirmed over wide temperature ranges.

3.2. Phase cooperation

The synergistic effect observed in the mixed oxide catalysts are generally known [15] to be from the three main reasons: (1) formation of new active phase by reaction between two phases, (2) increase of surface area, and (3) formation of mobile oxygen species and some chemical action of the latter (remote control mechanism). In order to understand the phase cooperation for V–Sb–O + Bi_2O_3 catalyst, the first possibility was verified by XRD method. The X-ray diffraction patterns of V–Sb–O + Bi_2O_3 (1:3) catalyst are presented in Fig. 2.

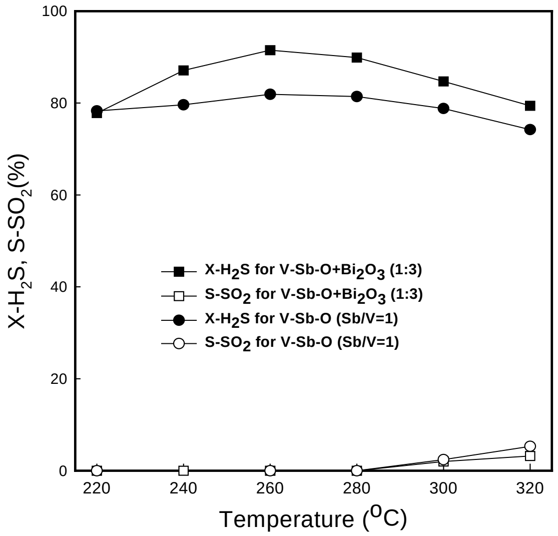

Fig. 1. Conversion of H_2S and selectivity to SO_2 for V–Sb–O + Bi_2O_3 (1:3) and V–Sb–O at different temperatures ($H_2S/O_2/NH_3/H_2O/He$ = 5/2.5/5/60/27.5, GHSV = 12,000 h^{-1}).

Fresh catalyst shows only characteristic peaks of $VSbO_4$ and Bi_2O_3. For the catalyst used for 8 h for the reaction, no new phase (principally $V_xBi_{1-x}O_y$) detectable by XRD was generated during the catalytic tests. Bismuth vanadates ($BiVO_4$, $Bi_4V_6O_{21}$) are reported to be one of the most active phases in coprecipitated V–Bi–O mixed oxide catalyst used in selective oxidation reaction [22–24]. Therefore, the increase of H_2S conversion for the mixture catalyst was not due to the formation of any new active site. Part of Bi_2O_3 was sulfided to Bi_2S_3. Secondly, BET surface areas of the fresh and used V–Sb–O + Bi_2O_3 (1:3) catalyst were measured and they were 1.69 and 1.13 m^2/g, respectively. The surface area of the fresh catalyst was nearly the same as the arithmetic average value of pure V–Sb–O (1.89 m^2/g) and Bi_2O_3 (0.69 m^2/g). The decrease in surface area of spent catalyst may be due

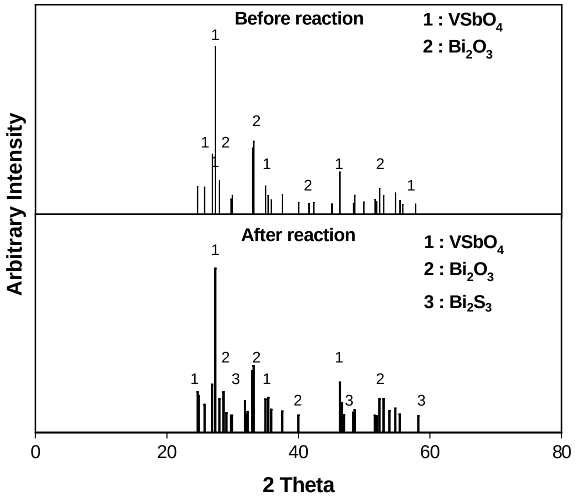

Fig. 2. XRD patterns of V–Sb–O + Bi_2O_3(1 : 3) catalyst before and after reaction.

to the increase of grain size. Therefore, the formation of new phase and increase of surface area can be excluded to explain the increase of H_2S conversion in this study. These two phenomena are generally accepted to be not evident to describe synergistic effect in mechanically mixed catalysts.

The role of mobile oxygen species is extensively studied to explain the phase cooperation in mechanically mixed catalysts. Weng and Delmon [15] reviewed remote control effects of two phases in several selective oxidation catalysts. This remote control mechanism supposes that a mobile oxygen species (spillover oxygen) is formed from gas phase oxygen on the surface of one phase and migrates onto the other, where it creates and/or regenerates the active centers. They also reported Bi_2O_3 could be a strong donor of mobile oxygen species. An attempt to verify the existence of the synergistic effect is to test the H_2S oxidation in two-bed operation modes. The H_2S conversions at three different operations for V–Sb–O+Bi_2O_3 (1:3) catalysts are summarized in Table 2. In case A, the reactant mixture is first contacted with V–Sb–O then Bi_2O_3 before it comes out of the reactor. The case B is the reverse of the order of case A. In case C, the uniform mixtures of V–Sb–O and Bi_2O_3 are placed together in the reactor. The operation in case C, where uniform mixing is obtained, showed higher H_2S conversion than cases A and B. The case B showed higher H_2S conversion than case A. One conclusion can be drawn from this result is that Bi_2O_3 is a donor phase and V–Sb–O is an acceptor phase for the mobile species, reaction intermediate or spillover oxygen.

Table 2
Conversion of H_2S and product selectivities for three different operations with V–Sb–O and Bi_2O_3 catalysts at 260 °C

	$X(H_2S)$ (%)	$S(SO_2)$ (%)	$S(S)$ (%)	$S(ATS)$ (%)
Case A: V–Sb–O → Bi_2O_3	81.0	0.0	72.3	27.7
Case B: Bi_2O → V–Sb–O	82.8	0.0	74.6	25.4
Case C: V–Sb–O + Bi_2O_3	89.9	0.0	75.8	24.2

In order to identify the real nature of this phase cooperation in V–Sb–O + Bi_2O_3 catalyst, TPR and TPO techniques are used in this study. A comparative temperature-programmed reduction (TPR) followed by temperature-programmed oxidation (TPO) were carried out for V–Sb–O, Bi_2O_3 and V–Sb–O + Bi_2O_3 (1:3), and the TPO results are shown in Fig. 3. The reducibility of the catalysts was first measured using TPR method with hydrogen as a reductant. In the subsequent TPO experiment, the mixture catalyst showed better reoxidation property than V–Sb–O and pure Bi_2O_3. The maximum peaks of O_2 consumption for the mixture catalysts were lower than V–Sb–O ($T_{max} = 600\,^{\circ}C$). The amount of hydrogen and oxygen consumed are summarized in Table 3. All the mixture

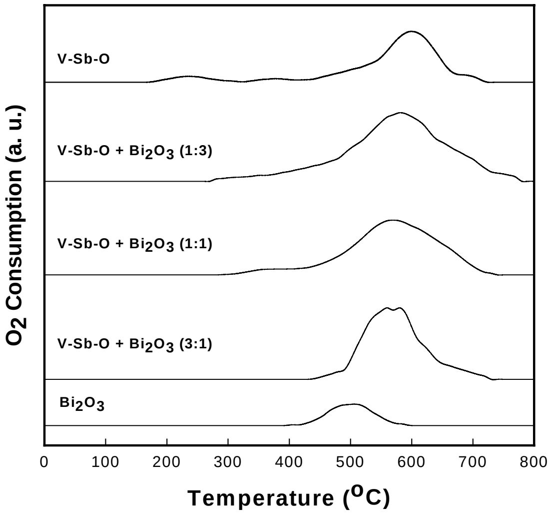

Fig. 3. TPO profiles of V–Sb–O, Bi_2O_3 and V–Bi–O + Bi_2O_3 catalysts.

Table 3
Desorbed amount of H_2 and O_2 in TPR and TPO experiments

Catalysts	H_2 (μmol/g_{cat})	O_2 (μmol/g_{cat})
V–Sb–O	26.53	52.44
V–Sb–O + Bi_2O_3 (3:1)	26.57	68.47
V–Sb–O + Bi_2O_3 (1:1)	28.90	73.97
V–Sb–O + Bi_2O_3 (1:3)	30.00	92.19
Bi_2O_3	38.44	15.29

catalysts showed higher amount of oxygen consumption than V–Sb–O and Bi_2O_3. V–Sb–O + Bi_2O_3 (1:3), the most active catalyst in Table 1, showed the highest amount of oxygen consumption. However, the amount of hydrogen consumption were not so different from others. Therefore, the increase of H_2S conversion in V–Sb–O + Bi_2O_3 mixture can be considered to come from the reoxidizing ability of Bi_2O_3.

The oxidation state of the vanadium in pure V–Sb–O and V–Sb–O + Bi_2O_3 (1:3) is studied by XPS. Fig. 4 shows XPS spectra of V $2p_{3/2}$ for the V–Sb–O and the mixture catalyst before and after 8 h of reaction at 260 °C with the standard reactant mixture and GHSV of 12,000 h^{-1}. The standard XPS peak of V $2p_{3/2}$ for V^{5+} and V^{4+} are located 516.9 and 515.6 eV, respectively. After the reaction, the XPS spectra were broadened and shifted to lower binding energy. It means that some of the fresh V–Sb–O having only V^{5+} state is reduced to V^{4+} after the reaction. The full-width half-maximum (FWHM) value for the fresh V–Sb–O was 1.15 eV, and that for the used V–Sb–O was 2.09 eV. It corresponds to 82.0% increase in FWHM after the reaction. However, the mixture catalyst showed 1.45 eV for the fresh catalyst and 2.15 eV for the used one, 48.3% increase in FWHM. Therefore, the mixture catalyst showed less reduction of vanadium oxide phase during the reaction. This can support the oxidizing ability of Bi_2O_3 for the mixture catalyst.

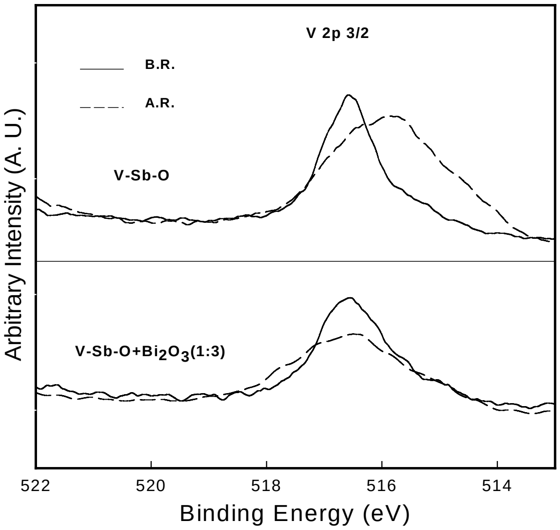

Fig. 4. XPS analyses of V–Sb–O and V–Sb–O + Bi_2O_3 (1:3) before (solid line) and after (dashed line) reaction: (H_2S—5 vol.%, O_2—2.5 vol.%, NH_3—5 vol.%, H_2O—60 vol.%, GHSV = 12,000 h^{-1}, and T = 260 °C).

A possible explanation for the synergistic effect of V–Sb–O + Bi_2O_3 mixture catalyst will be the following sequence of redox process. Since Bi_2O_3 is a p-type semiconductor, electron transfer can occur from V–Sb–O to Bi_2O_3 at the boundary of these two metal oxides. Then, oxygen vacancy can be formed and it will promote the dissociative adsorption of O_2. The oxygen ion O^{2-}, therefore, can reoxidize the partially reduced active phase of V–Sb–O.

4. Conclusions

The selective oxidation of hydrogen sulfide in the presence of excess water and ammonia was investigated in this study. Hydrogen sulfide was successfully converted into harmless ammonium thiosulfate and elemental sulfur without considerable emission of sulfur dioxide. Synergistic effects between V–Sb–O and Bi_2O_3 were observed for the mechanical mixtures of these catalysts. V–Sb–O + Bi_2O_3 (1:3) showed the most improved catalytic performance. TPO and XPS results supported the role of Bi_2O_3 for oxidizing the reduced vanadium oxide phase during the reaction.

Acknowledgements

This work was supported by the Korea Science and Engineering Foundation (R05-2003-000-10050-0), and the Brain Korea 21 and Brain Busan 21 programs.

References

[1] B.G. Goar, Oil Gas J. 25 (1975) 96.
[2] R. Lell, Sulphur 178 (1985) 29.

[3] Anon., Sulphur 231 (1994) 36.
[4] R. Lell, J.B. Novgayrede, Sulphur 213 (1991) 39.
[5] C. Dezael, L. Kerdaon, Rev. Int. Francois Petrole 49 (1994) 491.
[6] Anon., Sulphur 227 (1993) 39.
[7] R. Kettner, N. Liermann, Oil Gas J. 11 (1983) 63.
[8] R. Kettner, T. Liermann, European Patent 078,690 (1983), to Mobil Oil Corporation.
[9] P.J. Van den Brink, J.W. Geus, US Patent 5,352,422 (1994), to VEG-Gasinstituut N.V. and Comprimo B.V.
[10] P.J. Van den Brink, R.J.A.M. Terode, J.H. Moors, A.J. Van Dillen, J.W. Geus, in: P. Ruiz, B. Delmon (Eds.), Developments in Selective Oxidation by Heterogeneous Catalysis, Elsevier, Amsterdam, 1991, p. 123.
[11] P.F.M.T. Van Nisselrooy, J.A. Lagas, Catal. Today 16 (1993) 263.
[12] D.W. Park, S.W. Chun, J.Y. Jang, H.S. Kim, H.C. Woo, J.S. Chung, Catal. Today 44 (1998) 73.
[13] D.W. Park, B.K. Park, D.K. Park, H.C. Woo, Appl. Catal. A: Gen. 223 (2003) 215.
[14] K.T. Li, N.S. Shyu, Ind. Eng. Chem. Res. 36 (1997) 1480.
[15] L.T. Weng, B. Delmon, Appl. Catal. A: Gen. 81 (1992) 141.
[16] A. Zey, S. White, D. Johnson, Chem. Eng. Prog. 76 (10) (1980) 76.
[17] J.F. Benito, ES Patent 547,563 (1986).
[18] E.M. Hartley, M.J. Matterson, Ind. Eng. Chem. Fundam. 14 (1975) 67.
[19] B. Hsunling, B. Pratim, C.K. Tim, Ind. Eng. Chem. Fundam. 31 (1975) 88.
[20] K.H. Henke, G. Weiner, Ger. Offen. 2,635,649 (1978).
[21] D. Chang, M.C. McGaugh, US Patent 4,765,969 (1988).
[22] K.T. Li, M.Y. Huang, W.D. Cheng, Ind. Eng. Chem. Res. 35 (1996) 621.
[23] K.T. Li, C.S. Yen, N.S. Shyu, Appl. Catal. A: Gen. 156 (1997) 117.
[24] Y. Moro-Oka, Stud. Surf. Sci. Catal. 77 (1993) 95.